NASA TECHNICAL NOTE

NASA TN D-4759

NASA TN D-4759

NONCAVITATING AND CAVITATING PERFORMANCE OF TWO LOW-AREA-RATIO WATER JET PUMPS WITH THROAT LENGTHS OF 5.66 DIAMETERS

by Nelson L. Sanger

Lewis Research Center
Cleveland, Ohio

NATIONAL AERONAUTICS AND SPACE ADMINISTRATION • WASHINGTON, D. C. • AUGUST 1968

NONCAVITATING AND CAVITATING PERFORMANCE OF TWO LOW-AREA-RATIO WATER JET PUMPS WITH THROAT LENGTHS OF 5.66 DIAMETERS

By Nelson L. Sanger

Lewis Research Center
Cleveland, Ohio

NATIONAL AERONAUTICS AND SPACE ADMINISTRATION

For sale by the Clearinghouse for Federal Scientific and Technical Information
Springfield, Virginia 22151 – CFSTI price $3.00

ABSTRACT

Performance of two jet pumps was determined over a range of spacings of the nozzle exit from the throat entrance of 0 to 2.9 throat diameters. Maximum measured efficiencies of 31.3 and 37.6 percent were achieved for nozzle- to throat-area ratios of 0.066 and 0.197, respectively. These efficiencies were improvements over those obtained for previously investigated jet pumps with throat lengths of 7.25 diameters. A simple one-dimensional analysis predicted noncavitating performance within 2 percent at the best-efficiency conditions. The point of total headrise deterioration due to cavitation was predicted with reasonable accuracy by each of two related parameters.

CONTENTS

NONCAVITATING AND CAVITATING PERFORMANCE OF TWO LOW-AREA-RATIO WATER JET PUMPS WITH THROAT LENGTHS OF 5.66 DIAMETERS

by Nelson L. Sanger

Lewis Research Center

SUMMARY

The noncavitating and cavitating performance of two jet pumps with nozzle- to throat-area ratios of 0.066 and 0.197 was evaluated in a water facility. Both pumps evaluated had throat lengths of 5.66 diameters and diffuser included angles of 6°. The investigation was conducted to experimentally determine overall noncavitating and cavitating performance; to study the mixing characteristics over a wide range of geometrical and flow conditions; to compare the experimental results to those obtained for a previously investigated configuration with a throat length of 7.25 diameters and a diffuser included angle of $8^{\circ}6'$; and to compare the overall experimental performance to noncavitating theoretically predicted performance.

Experimental performance was obtained by operating two nozzles separately in a single test section. Spacing of the nozzle exit from the throat entrance was varied from 0 to 2.9 throat diameters. Deaerated, room-temperature, tap water was used as the test fluid.

Maximum measured efficiencies of 31.3 and 37.6 percent were achieved at area ratios of 0.066 and 0.197, respectively. These efficiencies constitute an improvement over those recorded for the pumps with throat lengths of 7.25 diameters and a diffuser included angle of $8^{\circ}6'$. Outlet static pressures were also improved by the reduction in throat length.

Noncavitating performance predicted at the fully inserted nozzle position by a one-dimensional analysis was within 5 percent for the 0.066-area-ratio pump, and within 10 percent for the 0.197-area-ratio pump, both at the best-efficiency flow conditions. At best-efficiency nozzle positions the same analysis predicted performance to within 2 percent for both area-ratio pumps.

The point of total headrise deterioration due to cavitation was predicted within reasonable accuracy by each of two related parameters. The jet pump configuration evaluated in this investigation represents a good compromise between optimum noncavitation and cavitation operation.

INTRODUCTION

The requirements of cavitation resistance, long-term dependability, and simplicity have resulted in the selection of the jet pump for several possible applications in liquid-metal Rankine-cycle electric power generation systems (refs. 1 and 2). One of the principal jet pump applications in Rankine-cycle systems is as an auxiliary boost pump for the radiator condensate pump. For such applications jet pumps with low ratios of nozzle exit to throat area (area ratio, R) are required. This requirement results from the combination of high boiler temperatures and pressures, low radiator temperatures and pressures, and a requirement for low jet pump power absorption.

There has been relatively little detailed investigation of low-area-ratio (<0.25) jet pumps. Furthermore, design of jet pumps for optimum noncavitating and cavitating performance is complicated by the large number of geometrical variables. The principal variables are throat length, spacing of the nozzle exit from the throat entrance, primary- and secondary-inlet contours, and diffuser geometry. The interrelation of some geometrical elements further compounds the problem of optimizing jet pump configurations for both noncavitating and cavitating operation.

In references 3 and 4 a jet pump with a throat length of 7.25 diameters was experimentally evaluated for two low area ratios, R = 0.066 and 0.197. Nozzle spacing was the only independent geometrical variable investigated. The relatively long throat permitted energy losses due to friction to grow at a faster rate than energy addition due to mixing near the throat exit. It was therefore concluded that a reduction in throat length would probably result in higher overall efficiencies.

In this investigation the performance of a jet pump with a shorter throat length, 5.66 diameters, was evaluated. Detailed investigations of the mixing characteristics and of overall cavitation and noncavitation performance were conducted for a wide range of operating conditions.

The noncavitation analysis developed in reference 3 and the cavitation prediction parameter developed in reference 4 were applied to the configurations and flow conditions investigated as a further test of their applicability in pumps with shorter throat lengths. Experimental results were compared directly with corresponding results from references 3 and 4.

Experimental performance at two area ratios (0.066 and 0.197) was obtained by operating two nozzles separately in a single test section. The test section was constructed with a circular bellmouth entry, a constant-diameter throat with a length of 5.66 diameters, and a diffuser with an included angle of 6°. The spacing of the nozzle exit from the throat entrance was varied between 0 and 2.9 throat diameters in both the noncavitating and cavitating investigations. Deaerated room-temperature (80° F (26.7° C)) tap water was used as the test fluid. Primary flow rates varied from 28 to

83 gallons per minute (1.77×10^{-3} to 5.24×10^{-3} m^3/sec), and secondary flow rates varied from 32 to 192 gallons per minute (2.02×10^{-3} to 12.12×10^{-3} m^3/sec).

PERFORMANCE ANALYSES

Principle of Operation

A schematic representation of a jet pump is shown in figure 1, and the symbols and nomenclature are presented in appendix A. The principle of operation of a jet pump is the transfer of energy and momentum from the high-velocity primary fluid to the pumped, or secondary fluid through a process of turbulent mixing.

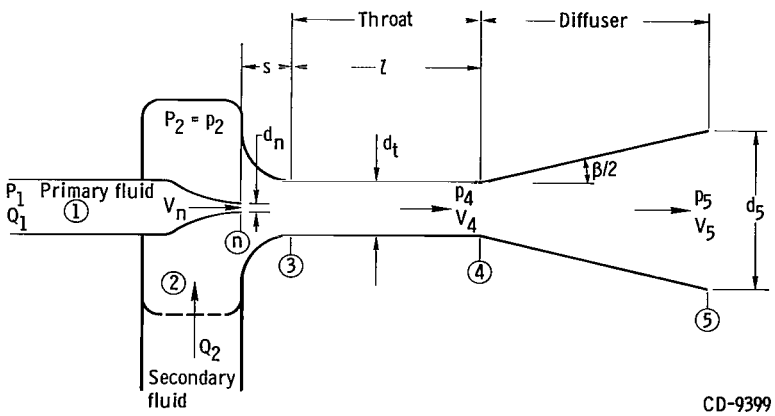

Figure 1. - Schematic representation of jet pump.

The primary fluid is pressurized by an independent source and is accelerated to high velocity in the nozzle. The secondary fluid is entrained by and mixed with the primary fluid in the throat or mixing section. The mixed fluids then pass through the diffuser in which a portion of the kinetic energy (velocity head) is converted to potential energy (static pressure).

The primary fluid leaves the nozzle as a core of high-velocity fluid. It is separated from the secondary stream by a thin region of high shear (see fig. 2). Turbulent mixing between the two fluids occurs in the mixing or shear region, which grows in thickness with increasing axial distance. The lowest local pressures occur in the shear region (ref. 5), and, therefore, cavitation inception also takes place in this region.

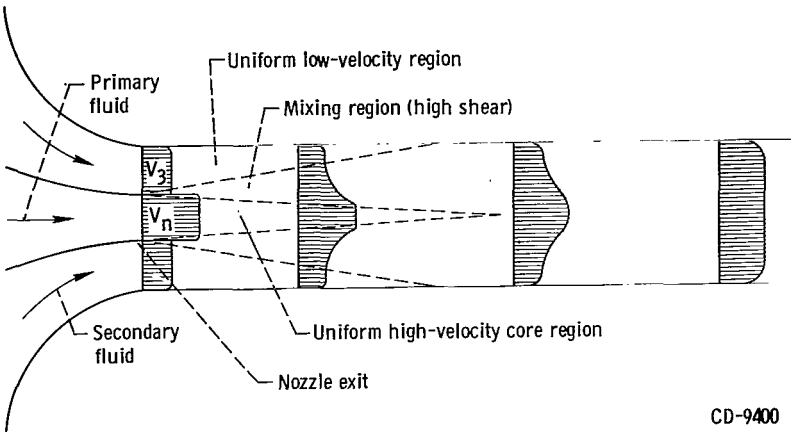

Figure 2. - Schematic representation of mixing velocity profile in throat of jet pump.

Analyses

The noncavitation and cavitation analyses presented in references 3 and 4 are one-dimensional and, therefore, somewhat limited in scope. Confined-jet mixing analyses (refs. 6 and 7) have not yet reached the stage whereby an easily applied jet pump design procedure can be derived. Thus, the one-dimensional analyses are generally used, but they must be supplemented by empirical information to determine optimum throat lengths, nozzle positions, diffuser geometry, and area ratios for specific applications.

Assumptions. - The following assumptions are common to both the noncavitation and cavitation analyses:

(1) Both the primary and secondary fluids are incompressible.

(2) The temperatures of the primary and secondary fluids are equal.

(3) Nozzle spacing from the throat entrance is zero.

(4) Nozzle wall thickness is zero.

(5) An additional assumption used in the noncavitation analysis is that mixing is complete at the throat exit.

Basic parameters. - There are four fundamental jet pump parameters, all expressed in dimensionless form. There parameters are

(1) Nozzle- to throat-area ratio, $R = A_n/A_t$

(2) Secondary to primary flow ratio, $M = Q_2/Q_1$

(3) Head ratio, $N = (H_5 - H_2)/(H_1 - H_5)$

(4) Efficiency, $\eta = MN$, the equivalent of net output power divided by net input power

A parameter that is useful in the study and comparison of axial static pressure variation in constant-diameter jet pumps is the pressure coefficient C_p defined by

$$C_p = \frac{p_x - p_2}{\gamma \frac{V_n^2}{2g}}$$

The numerator represents the pressure rise above secondary-inlet pressure at any axial location in the jet pump. The denominator is the velocity head of the primary fluid at nozzle exit. The use of this parameter permits direct comparison of data taken at different primary flow rates (i.e., different $V_n^2/2g$) and different secondary-inlet pressures.

Noncavitation analysis. - The noncavitation analysis is presented in detail in appendix B of reference 3 (Conventional Analysis). It consists of a one-dimensional application of the continuity, momentum, and energy relations across the individual components of the pump. Friction losses are taken into account through the use of friction loss coefficients K which are based on total pressure losses in individual components of the pump, such as the primary nozzle, throat, and diffuser.

The formula for head ratio N resulting from the analysis is

$$N = \frac{2R + \frac{2R^2M^2}{1 - R} - R^2(1 + M)^2(1 + K_t + K_d) - \frac{R^2M^2}{(1 - R)^2}(1 + K_s)}{1 + K_p - 2R - \frac{2R^2M^2}{1 - R} + R^2(1 + M)^2(1 + K_t + K_d)} \tag{1}$$

(All symbols are defined in appendix A, and determination of the various loss-coefficient values is discussed in appendix B.)

The formula for efficiency η is obtained by multiplying this expression for N by the flow ratio M.

Cavitation analysis. - The cavitation analysis (appendix B, ref. 4) applies to the conditions at the cavitation-induced total-headrise breakdown point, rather than to inception conditions. Although it is desirable to know the point of cavitation inception and the degree of cavitation that can be tolerated before performance loss is reached, the conditions at total-headrise breakdown most concern the designer.

The analysis presented in reference 4 consists of an application of the continuity and energy relations to the secondary fluid. Combined with this is the assumption that, when total head breaks down, the static pressure in the plane of the primary nozzle exit (and throat entrance) is equivalent to the vapor pressure of the fluid. The resulting nondimen-

sional expression for the cavitation prediction parameter is

$$\omega = \frac{P_2 - p_v}{\gamma \frac{V_n^2}{2g}} = \left(\frac{V_3}{V_n}\right)^2 (1 + K_s) = \left(\frac{MR}{1 - R}\right)^2 (1 + K_s) \tag{2}$$

at total-headrise dropoff. An alternate but closely related expression is

$$\alpha = \frac{P_2 - p_v}{\gamma \frac{V_3^2}{2g}} = 1 + K_s \tag{3}$$

at total-headrise dropoff. In reference 4 it was shown that the friction loss coefficient K_s could be neglected for nozzle spacings greater than 1 throat diameter, but that for nozzle spacings less than 1 throat diameter K_s had to be retained.

APPARATUS AND PROCEDURE

Test Pump

The test pump (fig. 3) consisted of the following elements: the primary nozzle, the secondary plenum, nozzle spacing shims, and the test section.

The stainless-steel plenum preceding the test section was $15\frac{1}{2}$ inches (39.35 cm) in diameter and had a capacity of about $4\frac{1}{2}$ gallons (1.70×10^{-2} m^3). Secondary fluid was supplied to it through two diametrically opposed 3-inch (7.61-cm) outside-diameter pipes.

The test section was fabricated from transparent acrylic plastic; a 5-inch (12.7-cm) circular-radius bellmouth, identical to that used in reference 3, was used as inlet to the throat.

In reference 3 a throat with a length of 7.25 diameters was used primarily as a means of studying the mixing characteristics in the throat. It was concluded that improvement in overall performance would probably ensue if a shorter throat, perhaps 5 to 6 diameters in length, were used. In accord with this the present test section was designed to have a throat with exactly the same diameter, 1.35 inches (3.43 cm), as the test section of reference 3 but with a length of 5.66 diameters.

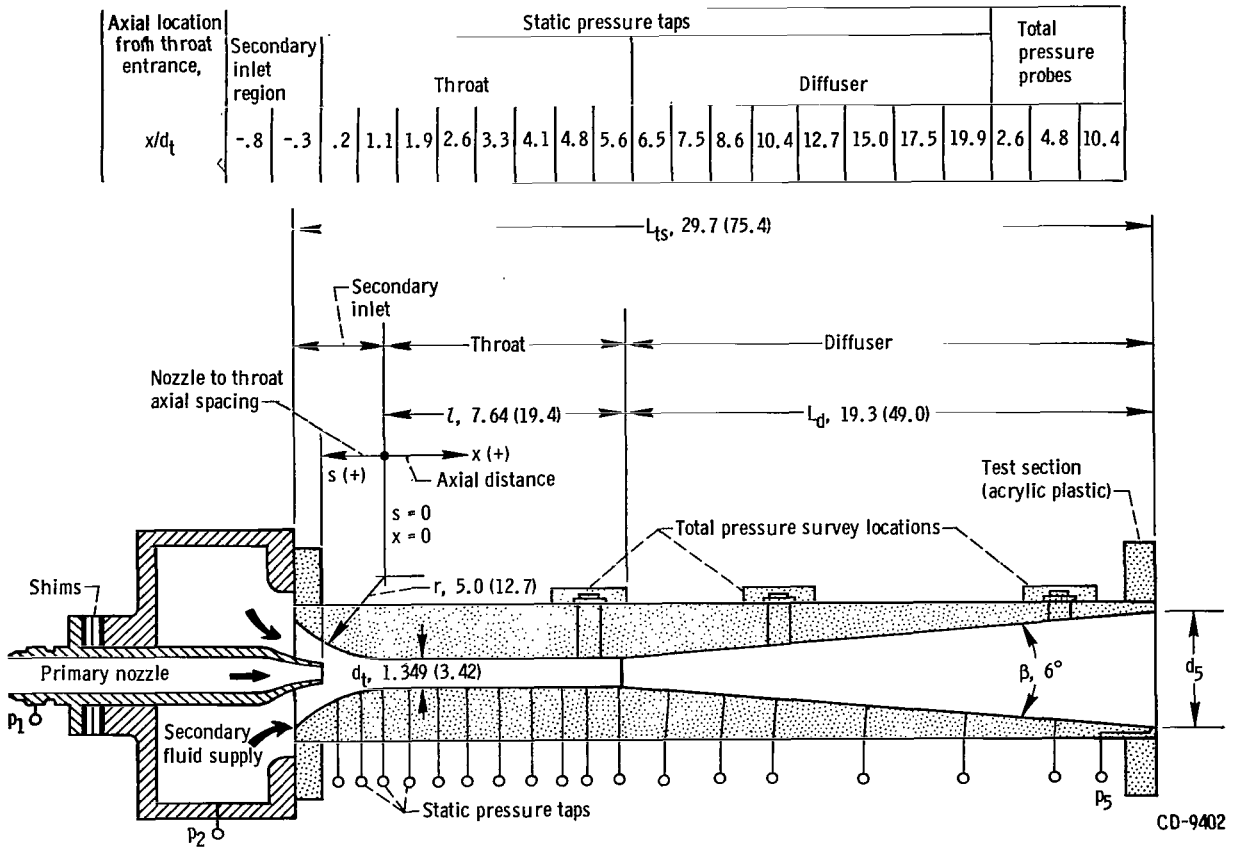

Figure 3. - Schematic diagram of test pump and location of static pressure taps and total pressure probes. (Diffuser area ratio, $(d_5/d_t)^2$, 6.25. (All dimensions are in inches (cm).)

A shorter throat may result in the continuation of some mixing in the upstream portion of the diffuser. The diffuser included angle was therefore reduced from the $8^{\circ}6'$ value of references 3 and 4 to a value of 6°, while the overall length of the jet pump was the same (29.7 in. (75.4 cm)). The diffuser outlet- to inlet-area ratio was thus fixed at 6.25.

Total pressure probes were mounted at axial locations of 2.6, 4.8, and 10.4 throat diameters measured from the throat entrance (see fig. 3).

Static pressure taps of 0.020 inch (0.051 cm) in diameter were installed at 18 axial locations (see fig. 3): two in the secondary-inlet region, eight in the throat, and eight in the diffuser. The two taps in the secondary-inlet region were drilled vertically and, thus, were inclined to the flow at angles of 15° and 5°, respectively. The errors introduced by such inclinations of static pressure orifices are considered negligible (ref. 8). Therefore, no corrections were applied to the static pressure data reported herein.

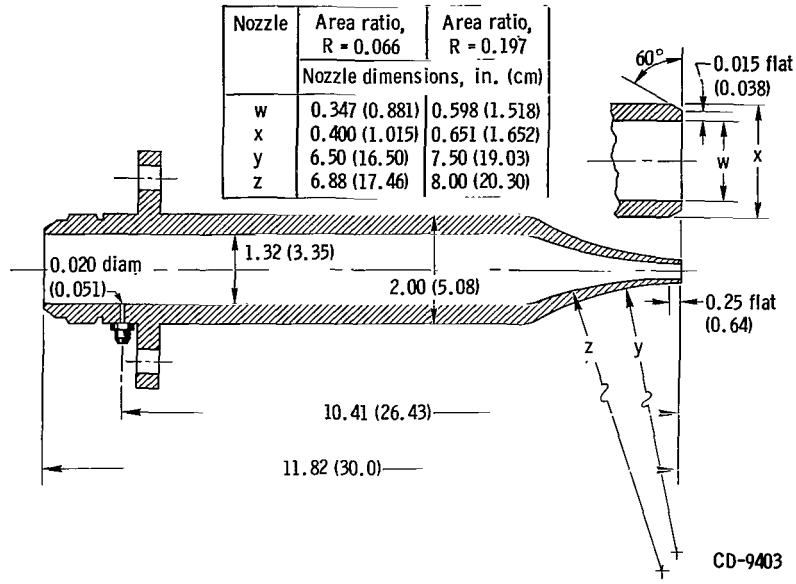

Figure 4. - Jet pump primary nozzles. (All dimensions are in inches (cm).)

Two stainless-steel primary nozzles, the same nozzles used in references 3 and 4, were operated separately in the test section. Their significant dimensions are shown in figure 4. The spacing of the nozzle exit from the throat entrance was controlled by the use of shims inserted between the nozzle flange and a reference surface on the plenum.

Apparatus

Test facility. - The test facility used in these tests is completely described in reference 3. A schematic diagram of the facility is shown in figure 5. The test facility was a closed-loop, continuous-circulation water tunnel with a total liquid capacity of about 350 gallons (1.325 m^3). The working fluid was deaerated tap water continuously filtered to remove particles larger than 25 micrometers.

Instrumentation. - The instrumentation used in this investigation is identical to that used in reference 3. Primary-fluid-inlet pressure was measured on a Bourdon tube gage. All other pressures used for data reduction were measured on mercury manometers. Primary and secondary flow rates were measured by turbine flowmeters. Total flow rate was measured by a venturi flowmeter. The venturi-measured flow rate agreed within ±2 percent of the sum of the primary and secondary flow rates.

Temperatures were measured in the primary, secondary, and mixed streams by means of copper-constantan thermocouples. Air content was measured with a Van Slyke gas apparatus.

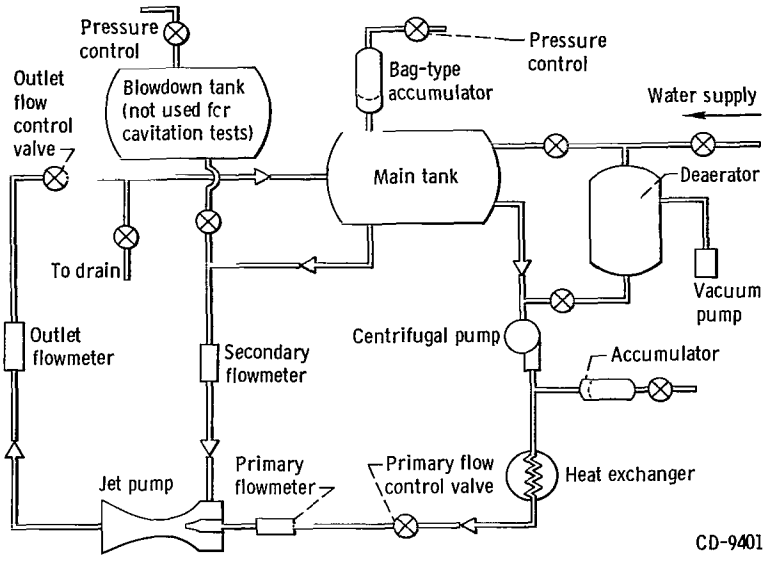

Figure 5. - Schematic drawing of water jet pump test facility.

The estimated error (instrument and readability combined) of the principal measured variables is as follows:

Headrise and static pressure, percent	$<\pm 0.7$
Inlet pressure (primary stream), percent	$<\pm 0.6$
Flow rate, percent:	
Primary stream	$<\pm 1.0$
Secondary stream	$<\pm 2.0$
Temperatures, ^{o}F (^{o}C)	$<\pm 2$ (1.1)
Total pressure surveys, percent:	
Total pressure	$<\pm 2.0$
Radial position	$<\pm 5.0$

Experimental Procedure

Testing method. - Performance was obtained over a wide range of operating conditions for both area ratios. The ranges of operation for both the noncavitating and cavitating tests are presented in table I.

Noncavitating test runs were conducted at constant values of secondary-inlet pressure and primary flow rate. Secondary flow rate, and, therefore, flow ratio, was varied.

TABLE I. - EXPERIMENTAL OPERATING VALUES

Area ratio, R	Nozzle spacing, s/d_t	Primary flow rate, Q_1		Flow ratio, M	Secondary inlet pressure, P_2	
		gal/min	m^3/sec		psia	N/m^2 abs
Noncavitating operation						
0.066	0 to 2.90	28	1.77×10^{-3}	1.15 to 5.64	15	1.03×10^5
.066	0 to 2.90	35	2.21	1.15 to 5.64	↓	↓
.197	0 to 2.66	63	3.98	.50 to 2.65		
.197	0 to 2.66	83	5.24	.50 to 2.65		
Cavitating operation						
0.066	0	28	1.77×10^{-3}	2.0 to 4.9	3.9 to 18.4	0.27×10^5 to 1.27×10^5
	.77	28	1.77	↓	↓	↓
	2.58	28	1.77			
	0	33	2.08			
	.77	33	2.08			
	2.58	33	2.08			
	0	35	2.21			
	.77	35	2.21			
	2.58	35	2.21			
0.197	0	63	3.98×10^{-3}	0.9 to 2.35	3.9 to 20.6	0.27×10^5 to 14.2×10^5
	1.36	63	3.98	↓	↓	↓
	2.66	63	3.98			
	0	75	4.74			
	1.36	75	4.74			
	2.66	75	4.74			
	0	83	5.24			
	1.36	83	5.24			
	2.66	83	5.24			

This procedure was followed at several nozzle positions for each area ratio. Total pressure surveys were also conducted at selected nozzle positions for each area ratio.

Cavitation performance was obtained at constant values of flow ratio. With flow ratio held constant as secondary-inlet pressure is reduced, head ratio remains constant at the noncavitating value until severe cavitation causes it to deteriorate.

Several values of flow ratio which spanned the best-efficiency point were selected. At each flow ratio, secondary-inlet pressure P_2 was reduced in discrete steps from a value corresponding to noncavitating operation until cavitation caused a sharp drop in total headrise.

Cavitation criteria. - In evaluating the cavitation performance of the jet pumps investigated, the following procedures were observed.

Air content: Space electric power systems will use liquid metals which have a low gas content. In order to simulate these conditions, the water in the jet pump test facility was deaerated to air contents of 3 parts per million or less.

Incipience: The flow conditions at total-headrise breakdown are of major interest for cavitating operation. Therefore, determination of incipient cavitating conditions was not emphasized. The secondary-inlet pressure was reduced slowly, and system variables were given time (approx. 1/2 to 1 min) to stabilize before data points were recorded. No attempt was made to increase the secondary-inlet pressure in order to define conditions at which cavitation disappeared (cavitation desinence).

RESULTS AND DISCUSSION

Noncavitation Performance

Overall performance. - Overall jet pump noncavitation performance is presented in figures 6 to 8 and is discussed in the following paragraphs.

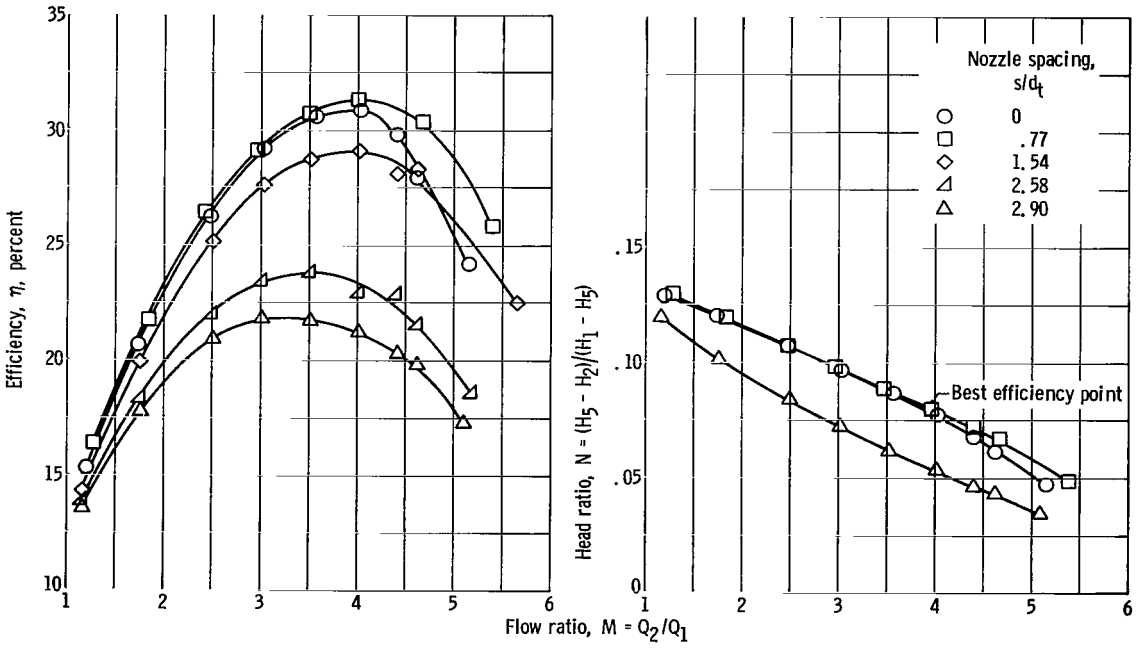

(a-1) Efficiency. (a-2) Head ratio.

(a) Area ratio, 0.066. Primary flow rate, 28 gallons per minute (1.77×10^{-3} m^3/sec).

Figure 6. - Noncavitating performance of jet pumps.

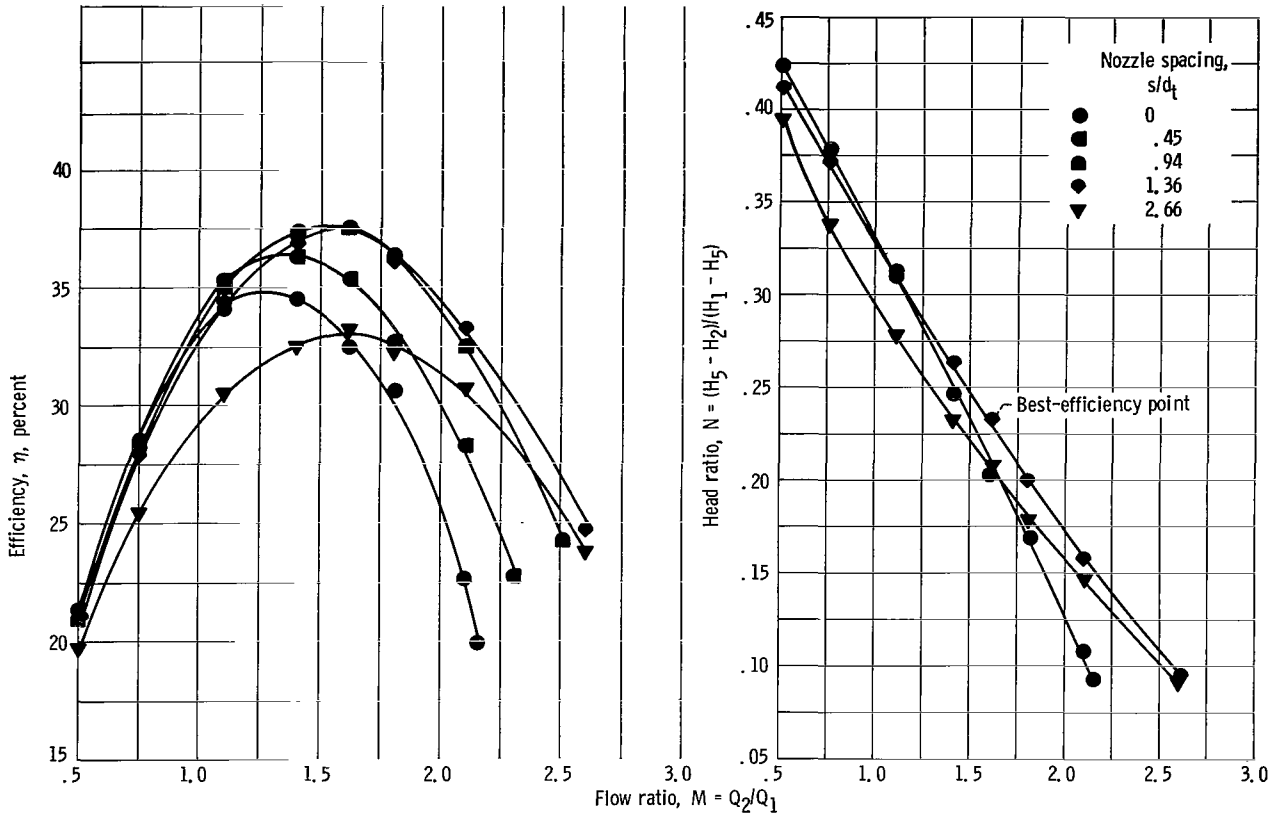

(b-1) Efficiency. (b-2) Head ratio.

(b) Area ratio, 0.197. Primary flow rate, 63 gallons per minute (3.97×10^{-3} m^3/sec).

Figure 6. - Concluded.

Efficiency and headrise: Jet pump overall noncavitation performance curves for area ratios of 0.066 and 0.197 are plotted as functions of flow ratio in figure 6. For the 0.066-area-ratio pump a peak measured efficiency of 31.3 percent was achieved at a nozzle spacing from throat entrance of 0.77 throat diameters, a head ratio of 0.079, and a flow ratio of 4.0. The 0.197-area-ratio pump achieved a maximum measured efficiency of 37.6 percent at a nozzle spacing s/d_t of 1.36, a head ratio of 0.233, and a flow ratio of 1.6. A reduction of throat length from 7.25 diameters (refs. 3 and 4) to 5.66 diameters resulted in an improvement in maximum efficiency from 29.6 to 31.3 percent for an area ratio of 0.066 and from 35.7 to 37.6 percent for an area ratio of 0.197. For both area ratios the best-efficiency condition occurred at larger nozzle spacings and larger flow ratios for the test pump with the shorter throat.

Values of headrise in feet (m) of water at selected flow conditions for $s/d_t = 0$ are presented in table II for both area ratios.

TABLE II. - JET PUMP HEADRISE FOR FULLY INSERTED

NOZZLE POSITION ($s/d_t = 0$)

[Secondary fluid inlet pressure, 15 psia (1.03×10^5 N/m^2 abs).]

Area ratio, R	Primary flow rate, Q_1		Secondary flow rate, Q_2		Jet pump headrise, $H_5 - H_2$		Flow ratio, M
	gal/min	m^3/sec	gal/min	m^3/sec	ft	m	
0.066	28	1.77×10^{-3}	33	2.08×10^{-3}	16.1	4.90	1.18
	28	1.77	99	6.25	10.4	3.17	3.53
	28	1.77	144	9.10	5.3	1.62	5.14
	35	2.21	33	2.08	24.8	7.56	.94
	35	2.21	89	5.62	19.2	5.85	2.54
	35	2.21	140	8.84	13.1	3.91	4.00
0.197	63	3.98×10^{-3}	31	1.96×10^{-3}	24.0	7.31	0.49
	63	3.98	88	5.55	14.2	4.32	1.40
	63	3.98	135	8.52	4.8	1.46	2.14
	83	5.24	42	2.65	41.7	12.7	.51
	83	5.24	91	5.75	30.6	9.32	1.10
	83	5.24	133	8.40	19.3	5.89	1.60

Best-efficiency nozzle position: Maximum pump efficiency as a function of nozzle spacing for the present test pumps and those of reference 3 are summarized in figure 7, in which three important effects are illustrated. First, the reduction of throat length from 7.25 to 5.66 diameters produced an improvement in maximum efficiency at practically every nozzle position. Second, the reduction in throat length resulted in an increase in the most efficient nozzle spacing. For a throat length of 7.25 diameters (ref. 3) the best-efficiency nozzle position was $s/d_t = 0$ at both area ratios. For a throat length of 5.66 diameters the best-efficiency nozzle positions (from fig. 7) were $s/d_t = 0.77$ and 1.36 for an area ratio of 0.066 and 0.197, respectively. This change in spacing is attributed to the fact that for the pump with the shorter throat the nozzle must be retracted a greater amount in order to provide the same degree of mixing. Third, the results for a throat length l/d_t of 5.66 also show an effect of area ratio on the most efficient nozzle position. The larger nozzle spacing required by the 0.197-area-ratio pump ($s/d_t = 1.36$) indicates that more mixing length was required by the larger-area-ratio pump. The same conclusion was reached in reference 3 from an analysis of the static and total pressure distributions.

One further remark should be made regarding figure 7. As was noted in references 9 to 11, the best-efficiency nozzle position is not sharply defined. Although a maximum efficiency may be identified, there is a certain degree of flexibility in selection of an operating nozzle position (fig. 7). This flexibility is particularly desirable because the

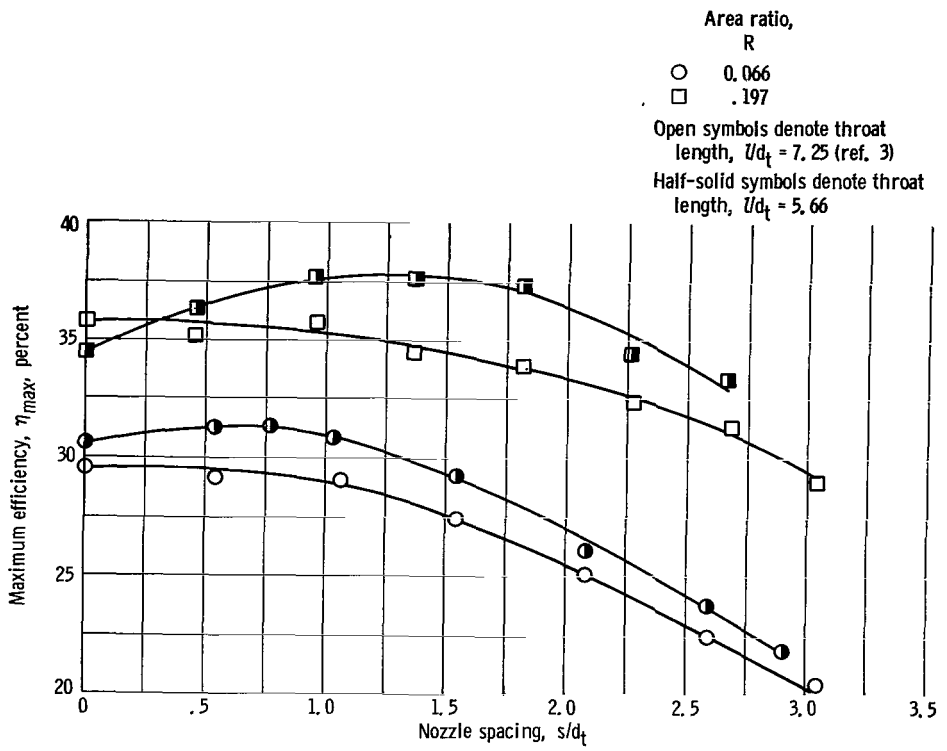

Figure 7. - Noncavitating jet pump performance. Effect of nozzle spacing on maximum efficiency.

best-efficiency nozzle position may not necessarily correspond to the best nozzle position from the standpoint of cavitation suppression (e.g., ref. 4).

Comparison of theory to experiment: In reference 3 the one-dimensional analysis (eq. (1)) was found to correlate head ratio and efficiency within 3 percent at the best-efficiency flow condition for both area ratios (0.066 and 0.197). Although based on an assumption of zero nozzle spacing, the theory predicted experimental performance between nozzle spacings of 0 and 1 throat diameter.

A similar comparison of theory to experimental results was made in the present investigation. In figure 8(a), the comparison is made at the fully inserted nozzle position ($s/d_t = 0$) for both area ratios. The agreement is considerably better at the best-efficiency nozzle position (fig. 8(b)) for both area ratios (within 2 percent at the point of maximum efficiency) than for the fully inserted nozzle position. At the latter condition, agreement is within 5 percent for $R = 0.066$ and within 10 percent for $R = 0.197$ at the maximum efficiency point. In general, agreement between theory and experiment was better than these values at flow ratios less than the best-efficiency flow conditions and worse at flow ratios greater than the best-efficiency flow conditions. The fully inserted nozzle position, coupled with a shorter throat length, apparently resulted in higher losses due to the continuation of some mixing into the inlet of the diffuser. Although based on an

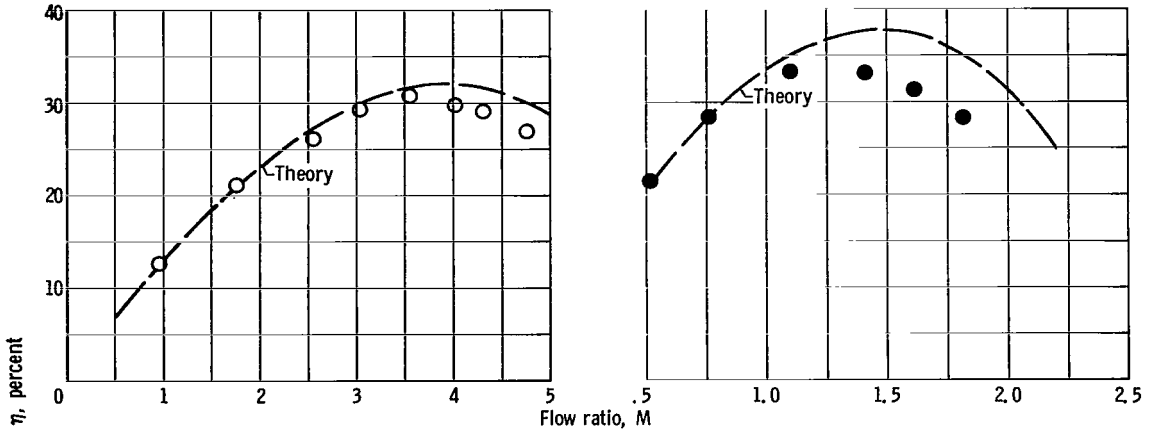

(a-1) Area ratio, 0.066; primary flow rate, 35 gallons per minute (2.21x10^{-3} m^3/sec).

(a-2) Area ratio, 0.197; primary flow rate, 83 gallons per minute (5.24x10^{-3} m^3/sec).

(a) Fully inserted nozzle position, $s/d_t = 0$.

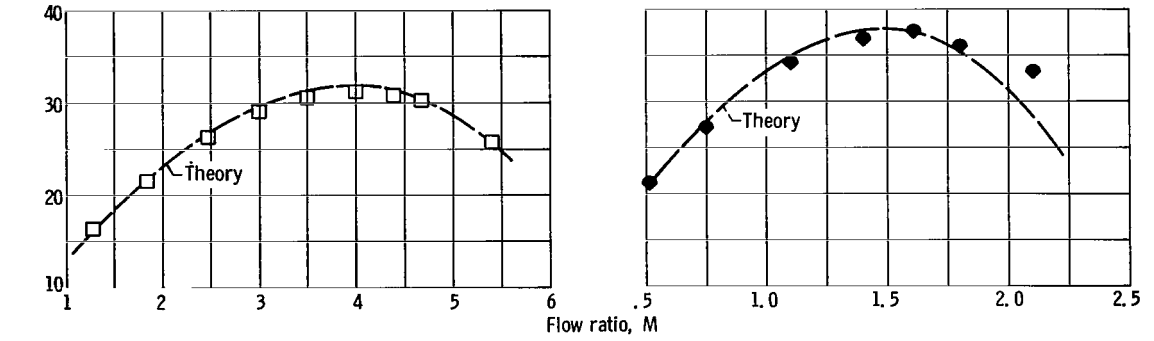

(b-1) Area ratio, 0.066; nozzle spacing, 0.77; primary flow rate, 28 gallons per minute (1.77x10^{-3} m^3/sec).

(b-2) Area ratio, 0.197; nozzle spacing, 1.36; primary flow rate, 63 gallons per minute (3.97x10^{-3} m^3/sec).

(b) At best-efficiency nozzle positions.

Figure 8. - Comparison of theory with experiment.

assumption of $s/d_t = 0$, the analysis did predict performance reasonably well between the zero spacing and best-efficiency nozzle spacing for both area-ratio pumps with throat lengths of $l/d_t = 5.66$.

Mixing characteristics. - The jet pump static and total pressure distributions are presented in figures 9 to 13 and are discussed in the following paragraphs.

Effect of flow ratio: The dimensionless static pressure distributions C_p are plotted in figure 9 as a function of axial location. The effect of flow ratio is shown for an area ratio of 0.066 at the best-efficiency nozzle position. Two effects are evident. As flow ratio is increased, overall pressure level decreases, and the rate of pressure increase in the throat decreases. These effects are independent of area ratio and were discussed previously in references 3 and 4.

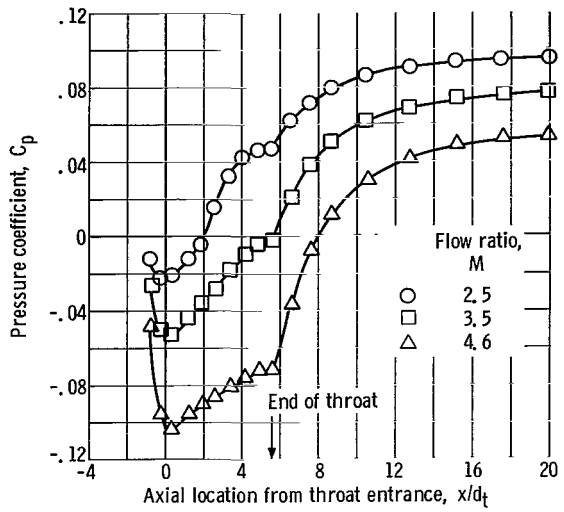

Figure 9. - Effect of flow ratio on axial static pressure distributions at best-efficiency nozzle position for area ratio of 0.066; nozzle spacing, 0.77.

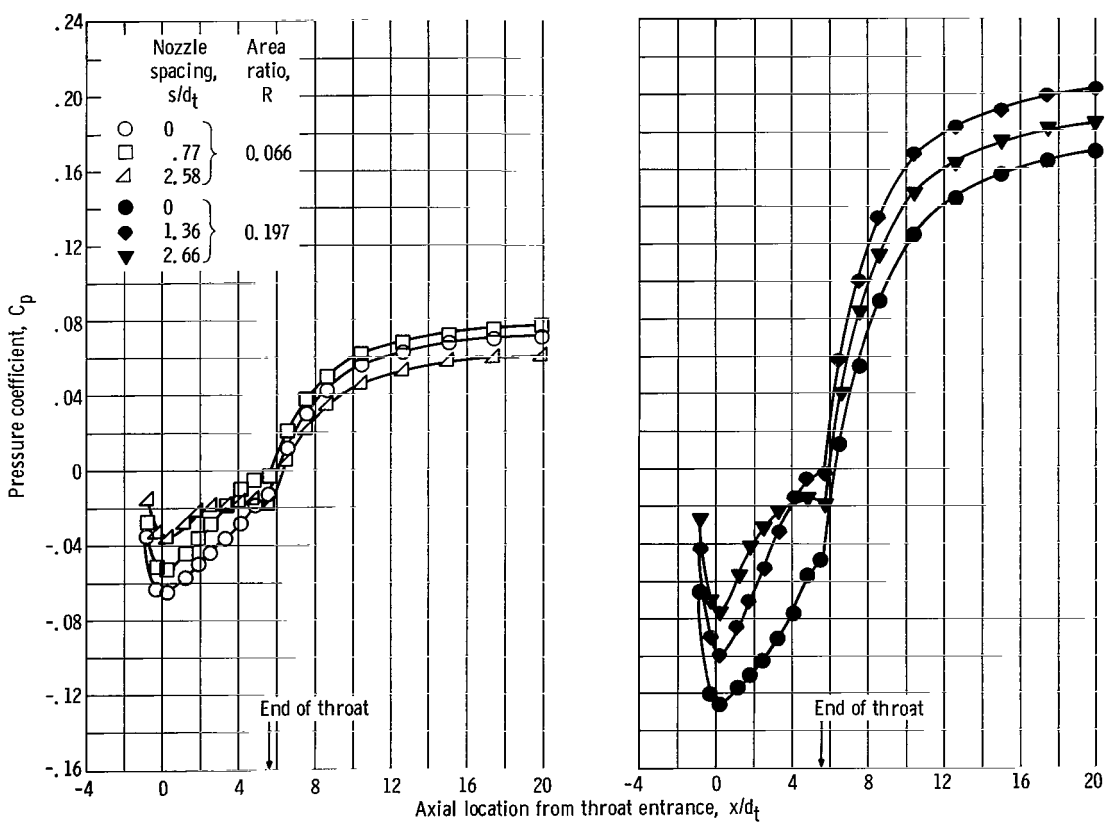

(a) Area ratio, 0.066; flow ratio, 3.5.

(b) Area ratio, 0.197; flow ratio, 1.4.

Figure 10. - Effect of nozzle position on static pressure distributions near best-efficiency flow ratio.

Effect of nozzle spacing: The wall static pressure distributions obtained for various values of flow ratio and area ratio at three nozzle positions are presented in figure 10. The three nozzle positions selected were the fully inserted nozzle position, the best-efficiency position, and a large nozzle spacing well into the low-efficiency range.

Two effects of nozzle spacing are evident at either area ratio: (1) as the nozzle is retracted, the static pressure level in the secondary-inlet and throat-inlet regions increases; and (2) at large nozzle spacings, static pressure decreased near the throat exit as a result of increasing frictional losses.

In figure 10, at the best-efficiency nozzle position for both area ratios ($s/d_t = 0.77$ for $R = 0.066$, and $s/d_t = 1.36$ for $R = 0.197$), the slope of the pressure increase in the throat began to show indications of leveling off near the throat exit. At the large nozzle spacings, static pressure decreased near the throat exit indicating that energy lost to friction was greater than the energy gained through mixing. Moreover, it appeared that more axial length was required by the 0.197-area-ratio pump to achieve a comparable amount of mixing than for the 0.066-area-ratio pump. At a nozzle spacing, s/d_t, of approximately 2.6, the static pressure increased rapidly in the 0.066-area-ratio pump, up to about two throat diameters from throat entrance. However, about four diameters were required for a comparable rise in the 0.197-area-ratio pump.

Total pressure surveys conducted at the three nozzle positions previously considered (fig. 10) for both area ratios are presented in figures 11 and 12. Axial static pressure distributions are also included in the figures. The surveys were conducted in the radial direction at three axial locations, denoted by the letters A, B, and C on the figures. The normalized total pressure $\mathscr{P}$ was obtained by dividing each local radial value of total pressure by the maximum value of total pressure (usually the midstream value). The normalized total pressure profile serves as a qualitative measure of the presence or absence of energy addition at a specific axial location.

No notable effect of flow ratio on the total pressure profiles was observed. Surveys for both area-ratio pumps show that, at all nozzle spacings, no mixing profile existed at the diffuser station ($x/d_t = 10.4$). Conversely, a mixing profile always existed at the first throat station ($x/d_t = 2.6$).

The mixing profiles which existed near the throat exit provide some insight into mixing length requirements. A distinct mixing profile existed near the throat exit for the fully inserted nozzle position. But it apparently did not strongly affect diffuser performance because the surveys at $x/d_t = 10.4$ were quite uniform. At the best-efficiency nozzle positions, less prominent mixing profiles existed near the throat exit. Static pressure had ceased to increase, indicating that, although some energy was being added through mixing action, about an equal amount was being lost due to wall friction. The result, therefore, was no net increase in static pressure. At the large nozzle spacings, some slight mixing action was apparent, but no distinct mixing profile existed at the

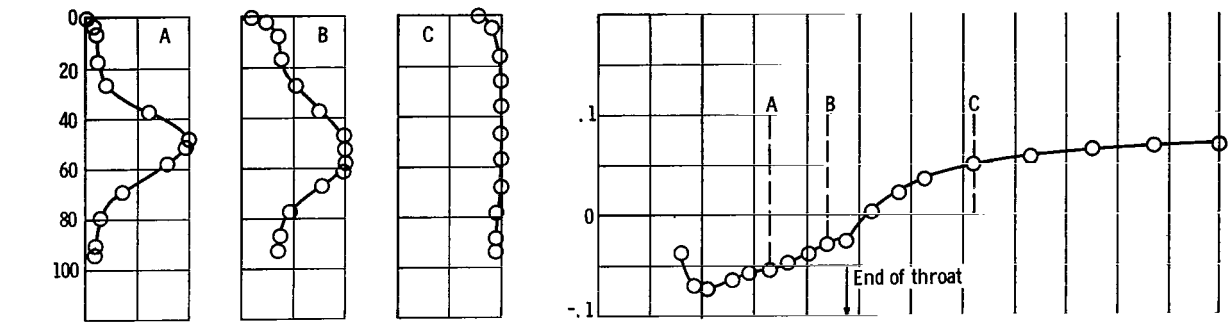

(a) Nozzle spacing, 0.

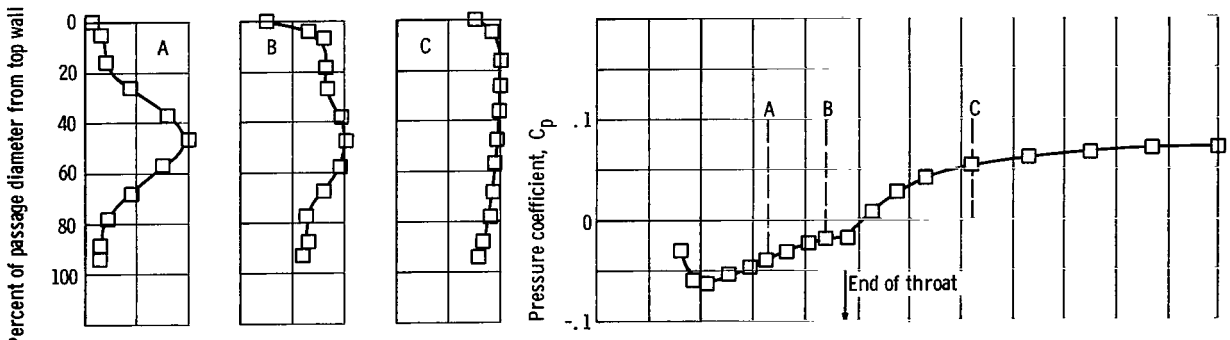

(b) Nozzle spacing, 0.77 (best-efficiency setting).

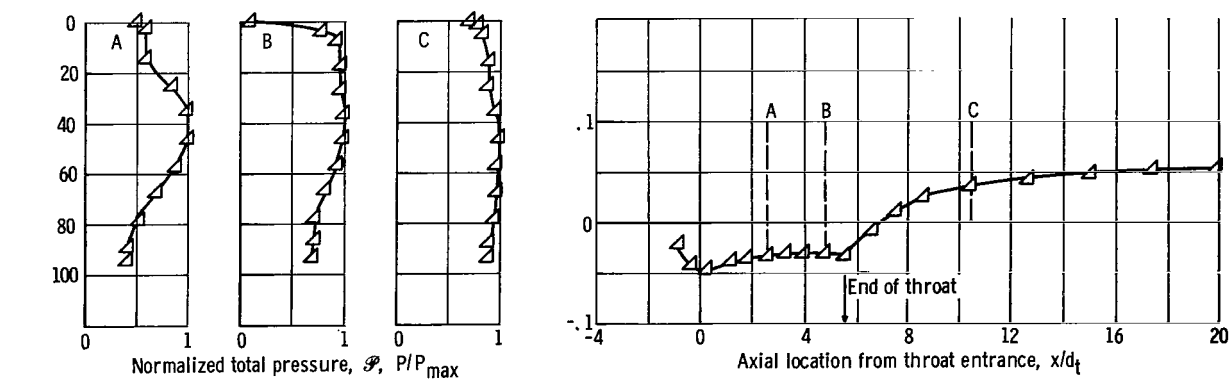

(c) Nozzle spacing, 2.58.

Figure 11. - Effect of nozzle position on mixing characteristics. Area ratio, 0.066; flow ratio, 3.75.

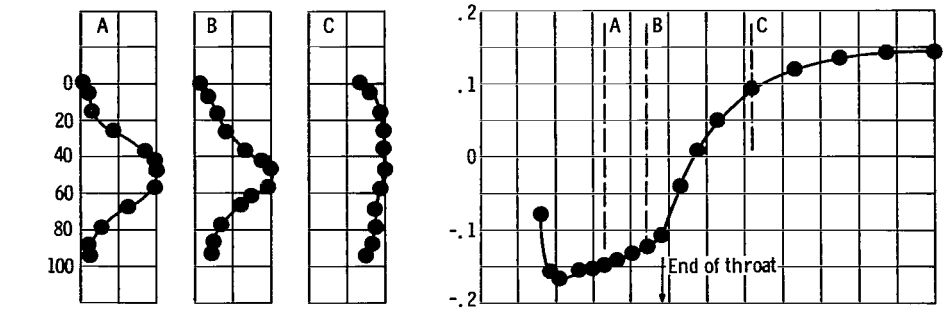

(a) Nozzle spacing, 0.

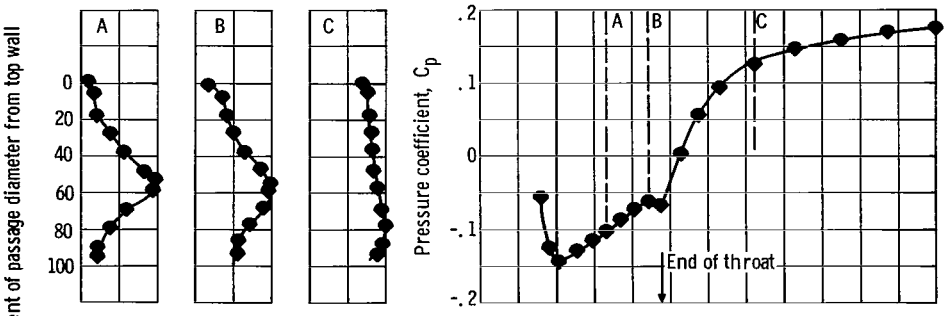

(b) Nozzle spacing, 1.36.

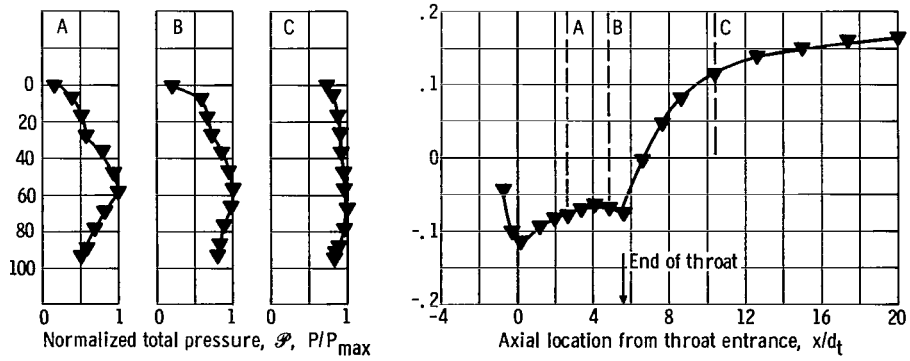

(c) Nozzle spacing, 2.66.

Figure 12. - Effect of nozzle position on mixing characteristics. Area ratio, 0.197; flow ratio, 1.6.

throat exit. The static pressure distributions for both area ratios indicated a loss in static pressure near the throat exit, denoting a predominance of friction losses over energy addition.

Effect of area ratio: In addition to an effect of nozzle spacing, figures 11 and 12 illustrate an effect of area ratio. A comparison of the total pressure profiles at the throat exit for similar nozzle positions reveals a more accentuated profile in the 0.197-area-ratio pump. That is, the larger-area-ratio pump required a greater axial distance to complete a comparable amount of mixing. This conclusion was reached earlier in the discussion of the axial distributions of static pressure and of the nozzle spacing required to produce maximum efficiency (fig. 7). A similar condition was observed in reference 3 for pumps with throat lengths of 7.25 diameters.

Because only two area ratios and one inlet configuration were evaluated, no general rule relating area ratio to required mixing length can be formulated. The effect is of a secondary nature, but nevertheless did produce different nozzle spacing requirements,

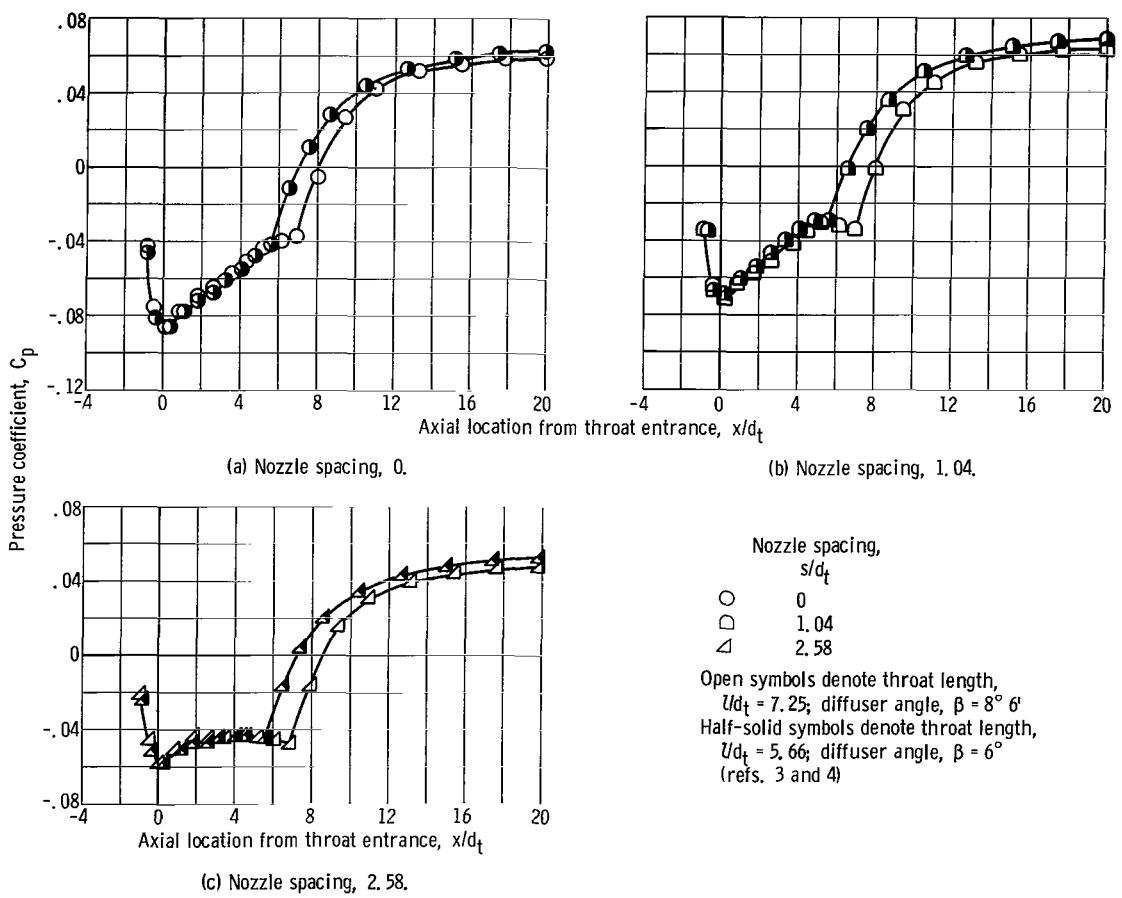

Figure 13. - Comparison of axial static pressure distributions for two jet pumps with different throat lengths. Area ratio, 0.066; flow ratio, 4.0.

and is important to the designer for that reason.

Effect of throat length: Static pressure distributions for jet pumps with throat lengths of 7.25 (ref. 3) and 5.66 diameters are compared in figure 13 for an area ratio of 0.066. Similar results were obtained at other flow conditions and for an area ratio of 0.197. The static pressure distributions for the two pumps compared quite closely in the secondary-inlet and throat regions, indicating that different downstream conditions of pressure and velocity did not affect the mixing characteristics in the constant-diameter section.

A reduction in throat length resulted, in most cases, in an improvement in overall pump static pressure rise as well as in efficiency. This is significant because efficiency is based on values of total pressure, and it is therefore not sine qua non that improvements in efficiency correspond in every instance to improvements in static pressure rise, or vice versa. Generalizations of this type should be avoided because the combination of overall static pressure rise and efficiency depends on specific diffuser geometry (included angle and area ratio) and throat length (inlet velocity profile to diffuser).

Due to the shorter throat length of the pump discussed in this report, a generally nonuniform velocity profile was provided to the diffuser. However, the diffuser had a smaller included angle (6° against $8^{\circ}6'$) and a smaller outlet- to inlet-area ratio (6.25 against 7.73) than the pump discussed in references 3 and 4. This produced a more gradual diffusion of kinetic energy and, apparently, as a direct consequence resulted in a higher static pressure rise. The mixing that occurred in the inlet to the diffuser was completed quickly and efficiently, judging from the static pressure distribution (figs. 11 and 12).

Cavitation Performance

Overall performance. - Cavitation performance is presented in figures 14 and 15 for both area ratios. Head ratio is plotted against net positive suction head H_{sv} of the secondary fluid. For each area ratio, the results are presented for one primary flow rate. The values of H_{sv} for which performance deteriorates are therefore applicable only for the stated conditions.

No performance dropoff is indicated for some of the low-flow-ratio conditions because the test-facility lower limit of secondary-inlet pressure, 9 feet (2.74 m) of water, was reached before cavitation dropoff occurred. (Arrows mark the approximate level at which visual incipiency was recorded.)

Effect of flow ratio: Figures 14 and 15 illustrate a distinct effect of flow ratio on net positive suction head required at headrise breakdown. These results are summarized in figure 16.

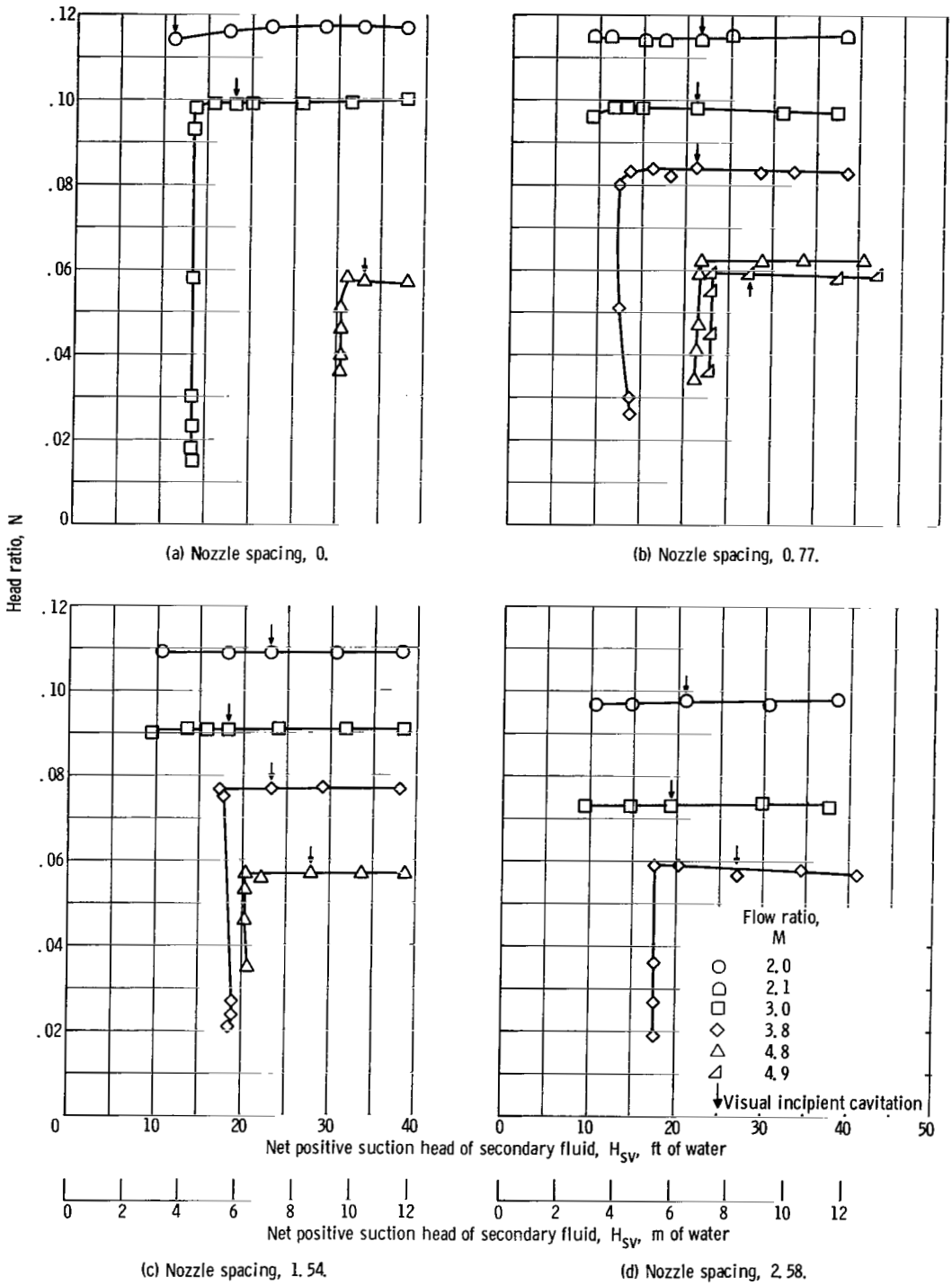

Figure 14. - Effect of inlet pressure and flow ratio on jet pump cavitation performance. Area ratio, 0.066; primary flow rate, 33.0 gallons per minute (2.08×10^{-3} m^3/sec).

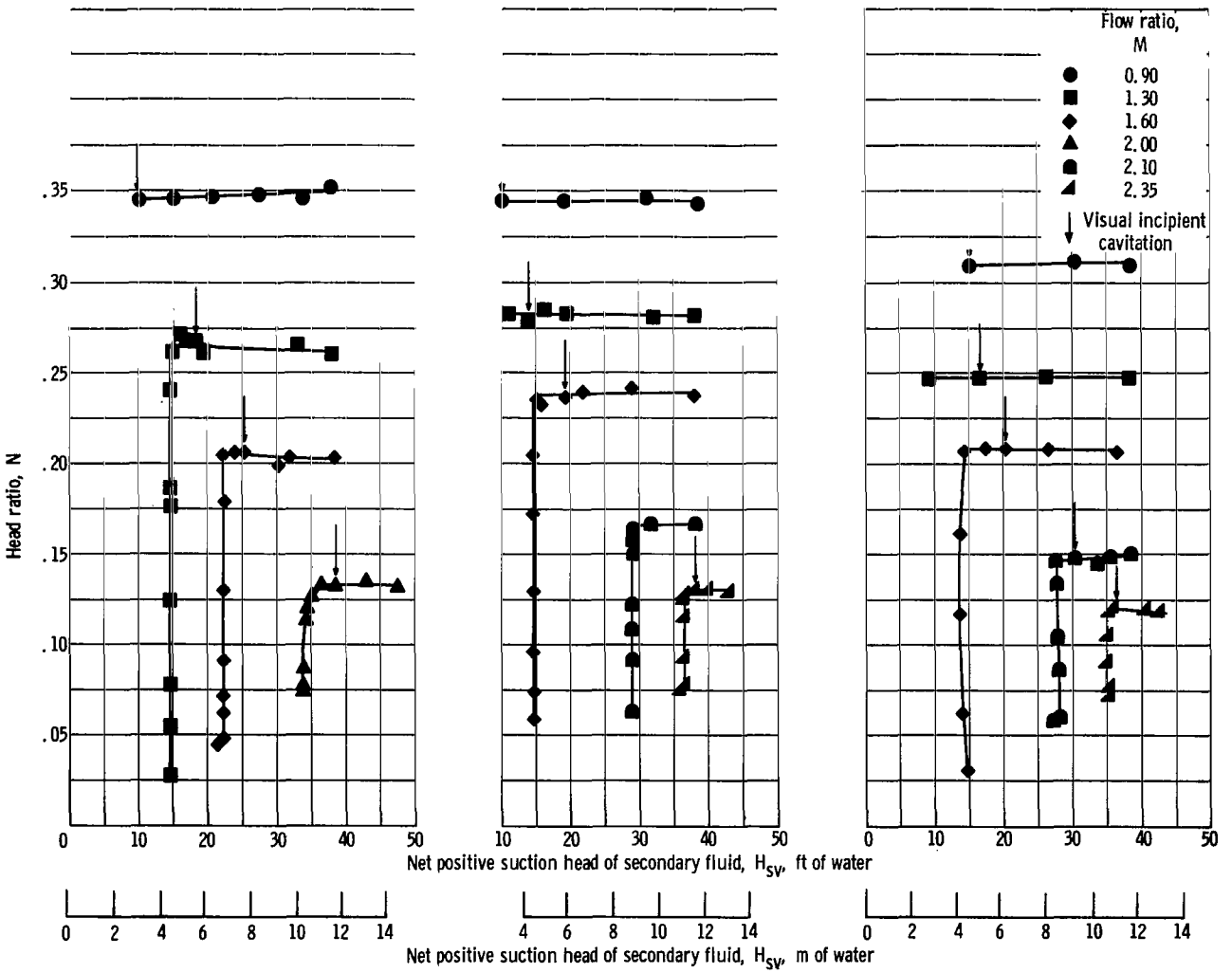

Figure 15. - Effect of inlet pressure and flow ratio on jet pump cavitation performance. Area ratio, 0.197; primary flow rate, 75.0 gallons per minute (4.74×10^{-3} m^3/sec).

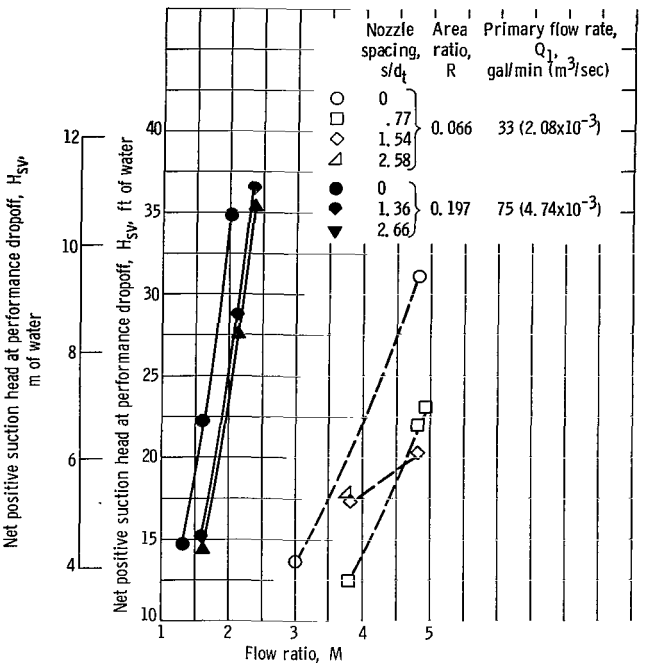

Figure 16. - Effect of flow ratio on required net positive suction head.

At a fixed nozzle position, higher secondary-fluid-inlet pressure was required as flow ratio was increased. As flow ratio is increased, cavitation becomes a greater problem because a higher flow ratio produces lower levels of static pressure in the inlet region of the pump (due to higher velocities) and a lower axial pressure gradient in the throat (fig. 9). Both effects act to sustain cavitation.

The best-efficiency flow conditions occurred near a point midway in the flow range of each pump (figs. 6(a) and (b)). The net positive suction head required at headrise breakdown for these conditions was only 12 to 15 feet (3.7 to 4.6 m) of water (fig. 16).

Effect of nozzle spacing: Figures 14 and 15 also show that required H_{SV} decreased as the nozzle spacing was increased at constant flow ratio. The effect is summarized in figure 17.

Except for a portion of one curve (M = 3.8) and perhaps only one point on the curve, the trends indicated by figure 17 suggest that to improve cavitation performance the nozzle spacings should be greater than 1 to $1\frac{1}{2}$ throat diameters. The same trend was observed in reference 4. Determination of an optimum operating nozzle position must take into account both cavitating and noncavitating operation (fig. 7). Comparison of cavitation and noncavitation data leads to the conclusion that if high efficiency and good cavitation performance were both design objectives, they could be achieved by operating the nozzle at a spacing of about 1 throat diameter for an area ratio of 0.066, and at about $1\frac{1}{2}$ throat diameters for an area ratio of 0.197.

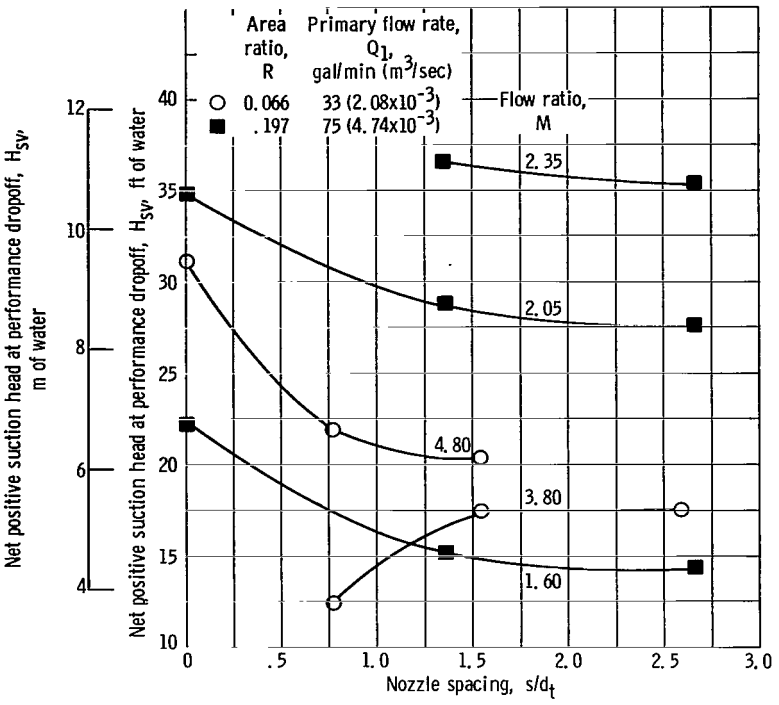

Figure 17. - Effect of nozzle spacing on required net positive suction head of secondary fluid.

Cavitation performance changes with nozzle spacing because retraction of the nozzle affects the static pressure distribution in the pump (fig. 10). For a constant flow ratio, as the nozzle was retracted the static pressure level in the throat increased. The retraction of the nozzle corresponds to an increase in the secondary annular area. For a fixed flow rate, an increase in area results in a decrease in velocity and an increase in static pressure.

A secondary factor which contributes to an increased susceptibility to cavitation at small nozzle spacings is the wake produced by the nozzle wall. This wake increases the turbulence in the mixing layer where cavitation occurs and has a greater influence at small nozzle spacings because the static pressure in the throat is low.

Prediction parameters. - Two related cavitation prediction parameters may be used to predict conditions at the jet pump headrise dropoff point.

Cavitation prediction parameter, ω: The parameter presented earlier (eq. (2)) was used to correlate the points of cavitation-induced total headrise dropoff for performance runs conducted at three primary flow rates at each area ratio. No effect of primary flow rate was observed. Typical results are presented in figure 18 for several nozzle positions at each area ratio. The parameter ω is plotted as a function of the ratio of secondary to primary fluid velocity at throat entrance V_3/V_n for various values of

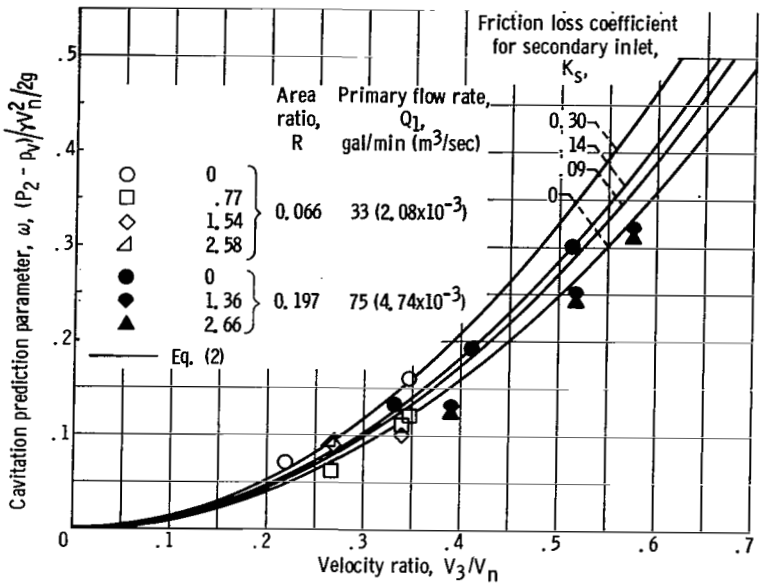

Figure 18. - Comparison of experimental jet pump cavitation results with prediction parameter, ω (eq. (2)).

secondary friction loss coefficient K_s (eq. (B2)). The values of K_s of 0.09 and 0.14 were measured in calibration tests for the area ratios of 0.066 and 0.197, respectively. The values of $K_s = 0$ and 0.30 were arbitrarily selected.

Comparison of experimental points to the theoretical curves reveals the same generally good correlation that was noted in reference 4. At the fully inserted nozzle positions, the values of ω at total headrise dropoff were slightly higher than theoretically predicted values for $R = 0.066$. The same trend was noted in reference 4. The differences were attributed to the effect of the wake produced by the nozzle wall in causing a greater susceptibility to cavitation and, hence, an earlier total-headrise dropoff. The higher values of ω for the 0.066-area-ratio pump as compared with the 0.197-area-ratio pump were attributed to its relatively thicker nozzle wake (8 percent of d_n compared with $4\frac{1}{2}$ percent of d_n, see fig. 4 (p. 8)). As both nozzles were retracted, the values of ω at total-headrise dropoff decreased because of the previously noted effects of nozzle spacing on the secondary-inlet static pressure field. For purposes of prediction, an empirical value of $K_s = 0$ may be used in equation (2) for nozzle spacings greater than or equal to 1 throat diameter. At smaller spacings, as suggested in reference 4, a value of K_s appropriate to the specific inlet configuration should be used.

Cavitation prediction parameter, α: An alternate parameter α which is related to the parameter ω was introduced in equation (3). Use of the parameter α eliminates the need to express jet pump cavitation performance in terms of the secondary- to primary-velocity ratio at throat entrance V_3/V_n. The cavitation performance data are

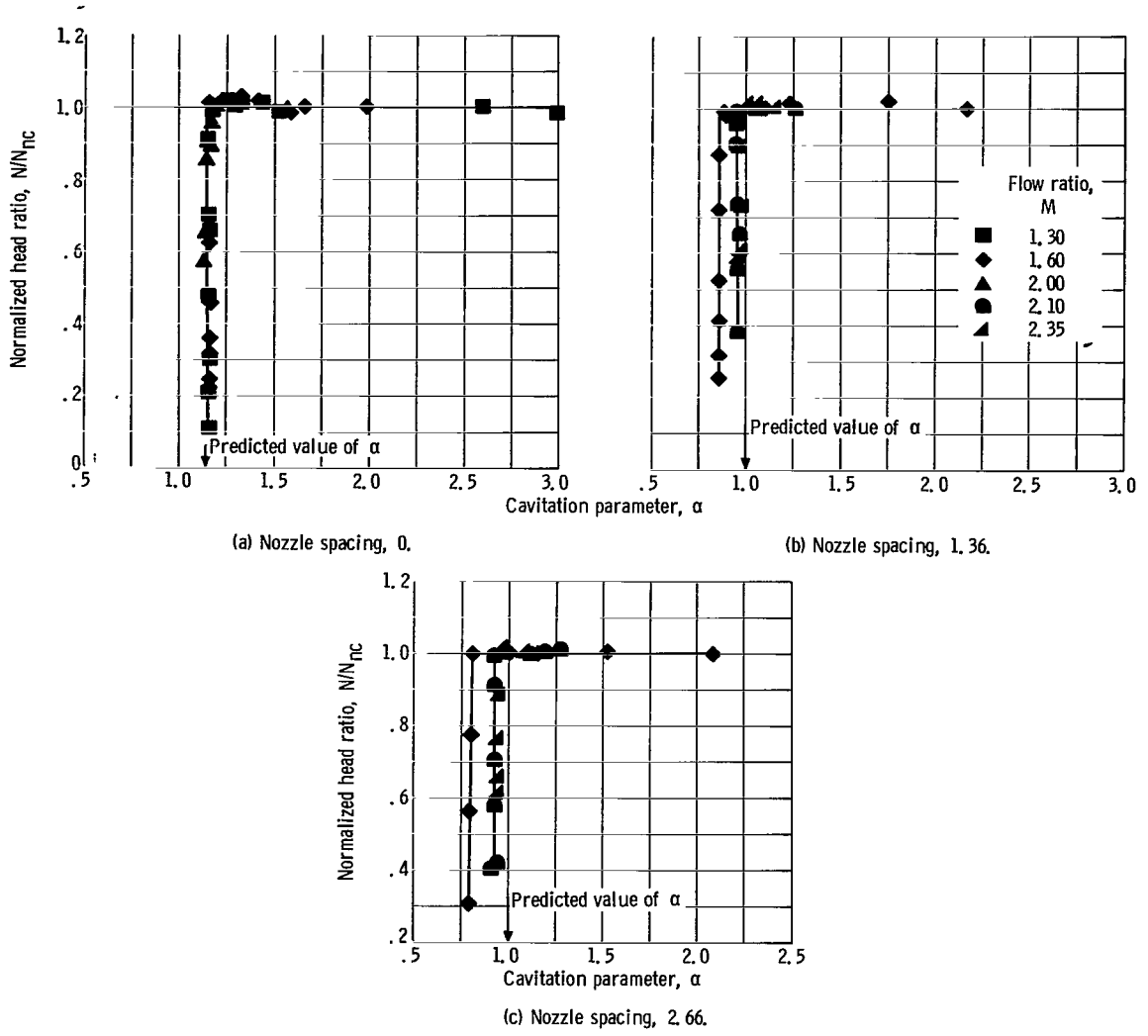

Figure 19. - Jet pump cavitation performance as function of cavitation parameter, α. Area ratio, 0.197; primary flow rate, 75 gallons per minute (4.74x10^{-3} m^3/sec).

presented in figure 19 for an area ratio of 0.197. The ordinate is a normalized head ratio, a ratio of operating head ratio N to the noncavitating value of head ratio N_{nc} at the specified flow conditions. Decreasing values of α indicate decreasing values of net positive suction head of the secondary fluid.

For a fixed nozzle position, the parameter α correlated the performance dropoff conditions with relatively good accuracy. Head ratio deterioration occurred at higher values of α (approx. 1.15 to 1.20) for the fully inserted nozzle position than for retracted nozzle positions (α, approx. 0.9 to 1.0). For purposes of prediction, the same values of K_s that were inferred from figure 18 for use with the formula for ω can be

inferred from figure 19 for use with the formula for α. This is not unexpected because of the relation, $\omega = \alpha(V_3/V_n)^2$.

SUMMARY OF RESULTS

The performance of two jet pumps with nozzle- to throat-area ratios of 0.066 and 0.197 and throat lengths of 5.66 diameters was evaluated in a closed-loop facility using room-temperature, deaerated water. Each nozzle was operated at nozzle spacings (distance nozzle exit is upstream from the throat entrance) of 0 to 2.9 throat diameters. Experimental results were compared with results from a previous investigation of two similar pumps with throat lengths of 7.25 diameters (refs. 3 and 4). Noncavitating performance was compared with performance curves predicted by a one-dimensional analysis; cavitating performance was compared with two related parameters also derived from a one-dimensional analysis.

The investigation yielded the following principal results:

1. For an area ratio of 0.066, a maximum measured efficiency of 31.3 percent was achieved at a flow ratio of 4.0 and a head ratio of 0.079. The maximum efficiency condition was attained at a nozzle spacing of 0.77 throat diameters. For an area ratio of 0.197, a maximum efficiency of 37.6 percent was achieved at a flow ratio of 1.6 and a head ratio of 0.233. The maximum efficiency was attained at a nozzle spacing of 1.36 throat diameters.

2. Compared with the jet pumps with throat lengths of 7.25 diameters, the 5.66-diameter-throat-length pumps produced higher efficiencies and outlet static pressures at practically every nozzle position. The reduction in throat length from 7.25 to 5.66 diameters also resulted in an increase in maximum-efficiency nozzle spacing.

3. The jet-pump configuration evaluated in this investigation represents a good compromise between noncavitation and cavitation operation. Both high efficiency and good cavitation resistance were achieved at a nozzle spacing of 1 throat diameter from throat entrance for an area ratio of 0.066, and at $1\frac{1}{2}$ throat diameters for an area ratio of 0.197.

4. At the fully inserted nozzle position, a one-dimensional analysis predicted noncavitation performance within 5 percent for the 0.066-area-ratio pump and within 10 percent for the 0.197-area-ratio pump, both at the best-efficiency flow conditions. For the best-efficiency nozzle settings, the same analysis predicted performance to within 2 percent for both area-ratio pumps at the best-efficiency flow conditions.

5. For a fixed nozzle position, higher secondary-inlet pressure was required to prevent cavitation as flow ratio was increased. For a fixed flow ratio, less secondary-

inlet pressure was required to prevent cavitation as nozzle spacing from the throat entrance was increased.

6. The point of performance deterioration due to cavitation was predicted with reasonable accuracy by each of two related parameters. To utilize these parameters it was necessary to consider an empirical loss coefficient for nozzle spacings between 0 and 1 throat diameter. It was possible to neglect this coefficient at larger nozzle spacings.

CONCLUDING REMARKS

In a previous investigation of jet pumps with throat lengths of 7.25 throat diameters, the matching of various geometrical components for optimum performance was discussed (ref. 3). Since there are many geometrical variables, several of which are interrelated, it is difficult to specify an "optimum" configuration.

However, the configuration evaluated in this investigation produced overall experimental results which indicated a good matching of components. The peak efficiency and head ratio compared well with the highest values reported in the literature. An interpretation of static and total pressure distributions indicated that the throat length is close to an optimum length and is matched well with the diffuser. A range of nozzle spacings was determined (around $s/d_t = 1.0$) at which both efficiency was maximized and net positive suction head requirements were reduced. Thus, for the designer seeking a jet pump configuration which produces high efficiency and satisfactory cavitation resistance, the configuration evaluated in this investigation might well be acceptable.

Lewis Research Center,
National Aeronautics and Space Administration,
Cleveland, Ohio, May 10, 1968,
128-31-06-28-22.

APPENDIX A

SYMBOLS

A	area, ft^2 (m^2)
C_p	pressure coefficient, $(p_x - p_2)/\gamma(V_n^2/2g)$
d	diameter, in. (cm)
f	Darcy friction factor
g	local acceleration due to gravity, 32.163 ft/sec^2 (9.803 m/sec^2)
g_c	dimensional constant, 32.174 ft lb mass/(sec^2)(lb force) (1.0 m kg/(sec^2)(N))
H	total head of fluid, P/γ, ft (m)
H_{sv}	net positive suction head of secondary fluid, $(P_2 - p_v)/\gamma$, ft (m)
h	static head of fluid, p/γ, ft (m)
K	friction loss coefficient
L	length, in. (cm)
ℓ	throat length, in. (cm)
M	flow ratio, Q_2/Q_1
N	head ratio, $(H_5 - H_2)/(H_1 - H_5)$
N/N_{nc}	normalized head ratio, ratio of operating head ratio to noncavitating head ratio
P	total pressure, lb force/ft^2 (N/m^2)
$\mathscr{P}$	normalized total pressure, P/P_{max}
p	static pressure, lb force/ft^2 (N/m^2)
p_v	vapor pressure, lb force/ft^2 (N/m^2)
Q	volumetric flow rate, gal/min (m^3/sec)
R	area ratio, $A_n/A_t = A_n/A_3$
s	axial spacing of primary nozzle exit from throat entrance, in. (cm)
V	velocity, ft/sec (m/sec)
x	axial distance measured from throat entrance, in. (cm)
α	cavitation prediction parameter, $(P_2 - p_v)/\gamma(V_3^2/2g)$, evaluated at total headrise dropoff due to cavitation
β	diffuser included angle, deg
γ	specific weight, g/g_c, lb force/ft^3 (N/m^3)
η	efficiency, MN
ρ	fluid density, lb mass/ft^3 (kg/m^3)
ω	cavitation prediction parameter, $(P_2 - p_v)/\gamma(V_n^2/2g)$, evaluated at total-headrise dropoff due to cavitation

Subscripts:

d	diffuser

n	primary nozzle exit plane
p	primary nozzle
s	secondary fluid inlet
t	throat
ts	test section
x	linear positions measured in axial direction from throat entrance

1	primary fluid
2	secondary fluid
3	location at throat entrance
4	location at throat exit
5	location at jet pump discharge (diffuser exit)

APPENDIX B

DETERMINATION OF FRICTION LOSS COEFFICIENTS

With the exception of the friction loss coefficient in the throat K_t, all friction loss coefficients were determined by experimental calibration.

Primary nozzle friction loss coefficient, K_p:

$$K_p = \frac{P_1 - p_n}{\gamma \frac{V_n^2}{2g}} - 1 \tag{B1}$$

A value of $K_p = 0.008$ was determined for the nozzle corresponding to an area ratio of 0.066; and a value of $K_p = 0.036$ for an area ratio of 0.197.

Secondary friction loss coefficient, K_s:

$$K_s = \frac{P_2 - p_3}{\gamma \frac{V_3^2}{2g}} - 1 \tag{B2}$$

For the fully inserted nozzle position, a value of $K_s = 0.09$ was determined for an area ratio of 0.066 and a value of $K_s = 0.14$ for an area ratio of 0.197.

Throat friction loss coefficient, K_t:

$$K_t = \frac{P_3 - P_4}{\gamma \frac{V_4^2}{2g}} = f \frac{l}{d_t} \tag{B3}$$

Reynolds numbers of the flow in the throat averaged 4.4×10^5. For a smooth pipe, this Reynolds number corresponds to a Darcy friction factor f of 0.0134. Therefore, $K_t = 0.076$.

Diffuser friction loss coefficient, K_d:

$$K_d = \frac{P_4 - P_5}{\gamma \frac{V_4^2}{2g}} \tag{B4}$$

The diffuser friction loss coefficient is also related to the diffuser efficiency by the expression

$$K_d = (1 - \eta_d)\left[1 - \left(\frac{A_4}{A_5}\right)^2\right] \tag{B5}$$

For fully retracted nozzle positions ($s/d_t \geq 2.7$), there is generally a uniform inlet velocity profile to the diffuser. The average diffuser efficiency determined for fully retracted nozzle positions was 90.6 percent. This efficiency corresponds to a value of $K_d = 0.079$. The components may be calibrated through individual flow calibration tests, as was done herein, or the friction loss coefficients may be estimated, based on values in the literature (refs. 9, 10, and 12).

REFERENCES

1. Sanders, Newell D.; Barrett, Charles A.; Bernatowicz, Daniel T.; Moffitt, Thomas P.; Potter, Andrew E., Jr.; and Schwartz, Harvey J.: Power for Spacecraft. Proceedings of the NASA-University Conference on the Science and Technology of Space Exploration. Vol. 2. NASA SP-11, vol. 2, 1962, pp. 125-150.
2. Chalpin, E. S.; Pope, J. R.; and Foss, C. L.: Development of a SNAP-8 Pump for Mercury Service. AIAA Specialists Conference on Rankine Space Power Systems. Vol. I. AEC Rep. CONF-651026, vol. 1, 1965, pp. 171-185.
3. Sanger, Nelson L.: Noncavitating Performance of Two Low-Area-Ratio Water Jet Pumps Having Throat Lengths of 7.25 Diameters. NASA TN D-4445, 1968.
4. Sanger, Nelson L.: Cavitating Performance of Two Low-Area-Ratio Water Jet Pumps Having Throat Lengths of 7.25 Diameters. NASA TN D-4592, 1968.
5. Rouse, Hunter: Cavitation in the Mixing Zone of a Submerged Jet. LaHouille Blanche, vol. 8, Jan.-Feb. 1953, pp. 9-19.
6. Curtet, Roger: Jet Flow Between Walls. Detailed Study of Ejector Pumps. Rep. RSIC-461, Redstone Scientific Information Center, Army Missile Command, Sept. 1965. (Available from DDC as AD-473568L.)
7. Pai, Shih-i: Fluid Dynamics of Jets. D. Van Nostrand Co., Inc., 1954.
8. Rayle, R. E.: Influence of Orifice Geometry on Static Pressure Measurements. Paper No. 59-A-234, ASME, 1959.
9. Cunningham, Richard G.: The Jet Pump as a Lubrication Oil Scavenge Pump for Aircraft Engines. Pennsylvania Univ. (WADC TR-55-143), July 1954.
10. Mueller, N. H. G.: Water Jet Pump. Proc. ASCE, vol. 90, no. HY3, pt. 1, May 1964, pp. 83-112.
11. Hansen, Arthur G.; and Kinnavy, Roger: The Design of Water-Jet Pumps. Part I - Experimental Determination of Optimum Design Parameters. Paper No. 65-WA/FE-31, ASME, Nov. 1965.
12. Gosline, James E.; and O'Brien, Morrough P.: The Water Jet Pump. Univ. California, Publ. in Eng., vol. 3, no. 3, 1934, pp. 167-190.

NASA-Langley, 1968 —— 12 E-4241

"The aeronautical and space activities of the United States shall be conducted so as to contribute . . . to the expansion of human knowledge of phenomena in the atmosphere and space. The Administration shall provide for the widest practicable and appropriate dissemination of information concerning its activities and the results thereof."

—NATIONAL AERONAUTICS AND SPACE ACT OF 1958

NASA SCIENTIFIC AND TECHNICAL PUBLICATIONS

TECHNICAL REPORTS: Scientific and technical information considered important, complete, and a lasting contribution to existing knowledge.

TECHNICAL NOTES: Information less broad in scope but nevertheless of importance as a contribution to existing knowledge.

TECHNICAL MEMORANDUMS: Information receiving limited distribution because of preliminary data, security classification, or other reasons.

CONTRACTOR REPORTS: Scientific and technical information generated under a NASA contract or grant and considered an important contribution to existing knowledge.

TECHNICAL TRANSLATIONS: Information published in a foreign language considered to merit NASA distribution in English.

SPECIAL PUBLICATIONS: Information derived from or of value to NASA activities. Publications include conference proceedings, monographs, data compilations, handbooks, sourcebooks, and special bibliographies.

TECHNOLOGY UTILIZATION PUBLICATIONS: Information on technology used by NASA that may be of particular interest in commercial and other non-aerospace applications. Publications include Tech Briefs, Technology Utilization Reports and Notes, and Technology Surveys.

Details on the availability of these publications may be obtained from:

SCIENTIFIC AND TECHNICAL INFORMATION DIVISION

NATIONAL AERONAUTICS AND SPACE ADMINISTRATION

Washington, D.C. 20546